

2012 AASRI Conference on Modelling, Identification and Control

## Tramway Track: a New Approach for Measuring the Transverse Profile of Worn-Out Rails

Marco Guerrieri<sup>a\*</sup>, Giuseppe Parla<sup>b</sup>, Dario Ticali<sup>c</sup>, Ferdinando Corriere<sup>d</sup>

<sup>a,c</sup> *Faculty of Engineering, University of Enna "Kore", Cittadella Universitaria, 94100 Enna, Italy*

<sup>b,d</sup> *Faculty of Engineering, University of Palermo, Viale delle Scienze, 90144 Palermo, Italy*

---

### Abstract

Monitoring the wear condition of the tramway superstructure is one of the key points to guarantee an adequate safety level of the light rail transport system. The purpose of this paper is to suggest a new non-conventional procedure for measuring the transverse profile of rails in operation by means of image-processing technique. This methodological approach is based on the "information" contained in high-resolution photographic images of tracks and on specific algorithms which allow to obtain the exact geometric profile of the rails and therefore to measure the state of the rail-head extrados wear.

© 2012 The Authors. Published by Elsevier B.V. Open access under [CC BY-NC-ND license](#).  
Selection and/or peer review under responsibility of American Applied Science Research Institute

*Keywords:* Tramway track, rails profile measurement, image analysis

---

### 1. Introduction

The rail wear and other imperfections on tramway track can be both monitored through low-efficiency equipment (e.g. miniprof device) or diagnostic trains which perform track laser scans while monitoring rail travels [1]. More recently the potentialities offered by *real-time image processing techniques* to determine the vertical, horizontal and 45° rail wear have been pointed out [2], [3], [4], [5], [6].

The following paragraphs describe the results got from laboratory analyses performed on worn-out rails taken from Tramway lines, and aimed to determine the transverse profile of the railhead by stereoscopic techniques applied on Grooved tram rail and UIC 60 rail.

---

\* Corresponding author. Tel.: +39 333.9993614.  
E-mail address: [marco.guerrieri@tin.it](mailto:marco.guerrieri@tin.it)

## 2. Image processing for tramwayrails profile measurement

The primary goal of image processing is to make the information content of a given image explicit with regard to the reference application type. All the segmentation methods are defined to process an image through specific algorithms which divide that image into distinct and uniform regions according to a set feature. This operation is the first step to distinguish the region enclosing the object of interest (ROI, region of interest) from the other parts or the background. After analyzing the image of the rail the segmentation procedure detects the image contour or “edge” through Canny’s algorithm [7]. Only afterwards this procedure solves the problem to compare the two rail profiles (worn-out and new) and to measure - for example - the vertical, horizontal and 45° deviations. The image edge detection phase is necessary in that digital images are definitely realized by high-resolution equipment but some image pixels could be affected by noise thus making the rail edge detection less accurate. More specifically, it is essential to detect the exact position of the image edge even in those parts where it cannot be distinguished, perceptually and/or numerically, from the clear background. Canny’s algorithm examines the behavior of the gradient operator applied to a noisy contour. The algorithm establishes that the pixel located at position  $(i,j)$  on the generic chromatic plane  $p^\dagger$  of the image  $A(i,j,p)$  is a Canny contour pixel if the intensity value of the pixel examined –  $A(i,j,p)$  – appears to be superior to given threshold values as established by Canny [7], based upon *hysteresisthresholding* and *non-maximum suppression* algorithms. The rail edge points obtained by Canny algorithm, denoted with  $\{C\}$ , are illustrated in the binary image of Fig. 2, which is an enlargement of a part of the original image (cf. Fig. 1). For each contour point  $\{C\}$  some clearer pixels which do not belong to rail microwrinkles can be detected near its edge. For every chromatic plane of the analyzed image, a median filter is applied by following this relation:

$$M=A*B \quad (1)$$

where *template B*, in this specific case, has a definite dimension  $[3 \times 3]$  and a coefficient equal to  $(1/9)$ .

$$B = \left(\frac{1}{9}\right) * \begin{bmatrix} 1 & 1 & 1 \\ 1 & 1 & 1 \\ 1 & 1 & 1 \end{bmatrix} \quad (2)$$

Relation (1) represents the pixel mean of the neighboring eight values. The implemented procedure iteratively applies the previous filter so as to spread the numerical values of all the pixels which certainly belong to a colorimetrically homogeneous region, located at either the background or rail. Therefore the idea is very simple: the image at time  $t$  (iteration step) derives from the initial image convolved with the median filter, or:

$$A(i,j,t) = A_0(i,j) \times M(i,j,t) \quad (3)$$

where  $(i,j)$  are the pixel position indices within the original matrix  $A$  and “ $\times$ ” represents the convolution operator. Moreover, since the expanded mean filter (3) tends to remove the information on the edge details, this effect should be mitigated by applying another operator which, instead, emphasizes the rail edge.

---

<sup>†</sup>“ $p$ ” is plane index:  $p=1$  Red plane,  $p=2$  Green plane,  $p=3$  Blue plane

In light of the above, downstream from the previous convolution (3), an edge extraction operator called *rangeoperator* was applied[8], [9]. For each deviation ( $i,j$ ) from template B, the value of the central pixel can therefore be formalized as follows:

$$R(i,j) = \text{Max}(A_{i-1,j-1}; A_{i-1,j}; A_{i-1,j+1}; A_{i,j-1}; A_{i,j}; A_{i,j+1}; \dots; A_{i+1,j+1} - \text{Min}(A_{i-1,j-1}; A_{i-1,j}; A_{i-1,j+1}; A_{i,j-1}; A_{i,j}; A_{i,j+1}; \dots; A_{i+1,j+1}) \quad (4)$$

To this end the range values of every  $[3 \times 3]$  boundary of all the pixels belonging to the original image A have been sought and highlighted. The following equation (5) formalizes the previous difference operation. Therefore, given a generic iteration step  $t$ , the suggested algorithm is able to lower the pixel intensities which mark the rail edge of the plane section.

$$\text{Min}(A_{i-1,j-1}; A_{i-1,j}; A_{i-1,j+1}; A_{i,j-1}; A_{i,j}; A_{i,j+1}; \dots; A_{i+1,j+1}) \quad (5)$$

It can easily be noticed that, with regard to any direction taken along the rail edge, while relation (3) tends to make numerically uniform the pixel value on the point edge under consideration, relation (4) on the same boundary lowers the values in the darkest regions and therefore colorimetrically near the rail.

Then we detected some uncertainty areas along the point edges where the profile in the eight directions marked a rough variation or, in any case, a skip over a precise threshold level, localized by three constants  $[T_i, T_o, T_s]$ . Such constants are automatically determined by the algorithm in relation to the maximum, minimum and mean deviation values of the two profiles. In these areas, for each iterative step  $t$  the pixel values fill in the matrixes  $\{S_i\}$  and  $\{G_i\}$ , well distinct from the matrixes  $\{S\}$  and  $\{G\}$  which instead are almost certainly background and rail. Therefore, at the iterative step  $t$  we have:

$$S(i,j,t) = J(i,j,t, T_i) \quad (6)$$

$$S_i(i,j,t) = J(i,j,t, T_i, T_o) \quad (7)$$

$$G_i(i,j,t) = J(i,j,t, T_o, T_s) \quad (8)$$

$$G(i,j,t) = J(i,j,t, T_s) \quad (9)$$

The suggested algorithm is able to define the matrix  $CF(i,j)$  of the final edge, which is formalized by the following relation:

$$CF(i,j,t) = F(S(i,j,t), S_i(i,j,t), G_i(i,j,t), G(i,j,t)) \quad (10)$$

where  $F$  is the function which formalizes the belonging of the pixel to the rail boundary or to the background. Its superimposition on the original image is illustrated in Figure 5.



Fig.1. Grooved Tramway Rail image



Fig.2. Binary image

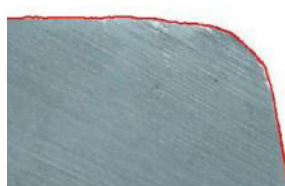


Fig.3. Final result of the algorithm suggested

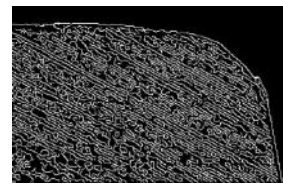


Fig.4. Binary encoding of the previous rail part

It should be underlined that, downstream from the previous thresholding operations (cf. eq. 9), the procedure is also able to extrapolate not only the exact contour position (cf. eq.10), but also a first object-based binary encoding which is formalized as follows:

$$G(i, j, t) = J(i, j, t, Ts) \quad (11)$$

The result which can be obtained by applying the previous relation to the rail part in Fig.1, is illustrated in Fig. 4. This binary encoding is properly refined on the basis of some binary morphology operations. In fact, by carefully examining Figure 4 we note that this binary selection has inside some cavities which do not allow to create a *binary large object* or *blob* constituted by close and connected pixels; therefore it requires the application of some mathematical morphology operations [10] which allow to modify the original information and to obtain the matrix BW illustrated in Fig.5 with regard to the whole rail image, which clearly shows a complete connectivity between neighboring pixels.



Fig.5. Morphological Closing Operations for the rail under examination

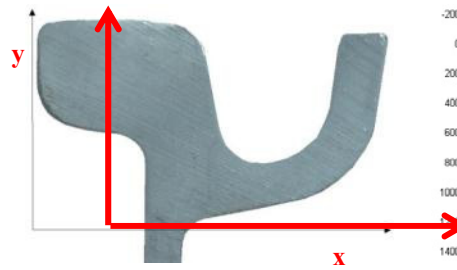


Fig.6. Cartesian coordinate system for Grooved rail

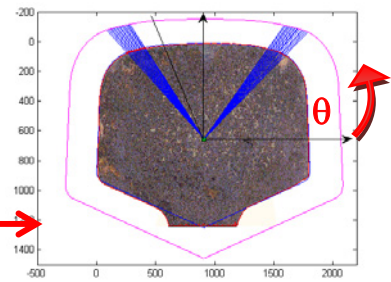


Fig.7. Polar coordinate system for UIC Rail

### 3. Results and discussion

For the purpose of this research, we further measured some geometrical sizes which characterize the binary object shape previously defined. The most widespread method to encode a binary object edge, originally developed by Freeman [11], is commonly known as *chaincode* and consists in storing a list of points. Once determined the coordinates of a point in the object border, the successive point is detected only by following the direction which connects pixel barycentres [12]. Therefore, once detected the blob (binary large object) and its contour coordinates, it is simple to calculate the centroid (M) representing the center of mass (center of gravity). We then could determine the centroid position ( $x_{oj}$ ,  $y_{oj}$ ) of the worn-out rail and its contour coordinates, by means of Freeman's algorithm developed on the result formalized by relations (10) and (11) after carrying out, as said above, the proper morphological closing operations (cf. Fig.5). These coordinates are properly recorded in the vector *WR* (*worn-out rail*) of dimension  $[n \times 2]$ , where  $n$  is the Cartesian axis number of the edge. The algorithm then adds the profile coordinates of the unworn rail (Grooved rail and UIC 60 rail have been taken into consideration) and carries them to the same image scale previously determined. For the UIC 60 rails the distances between the two profiles have been determined by the intercepts of the straight lines from the centroid of the profile *IR*, with regard to this last boundary *Rg*, whose domain is obviously perfectly parallel to the previous one. The procedure allows to get the deviation between the two compared profiles (worn-out and unworn) with regard to a 360° rotation of the straight line coming out of the rail centroid and, therefore, produces output information on the wear condition of the whole rail profile [3],[4], [13], [14]. The following diagrams illustrates the trend of the deformation of a Grooved rail and UIC 60 rail.

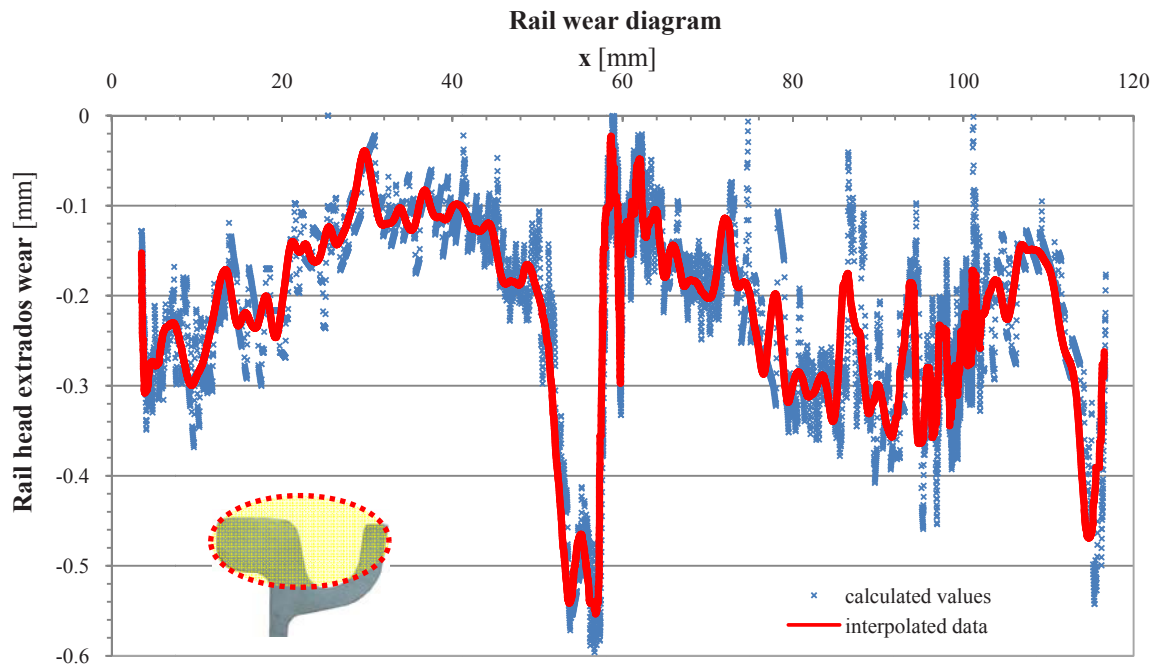
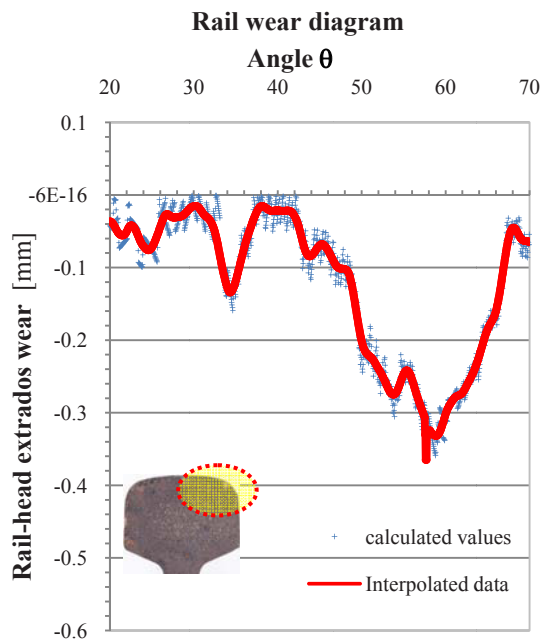
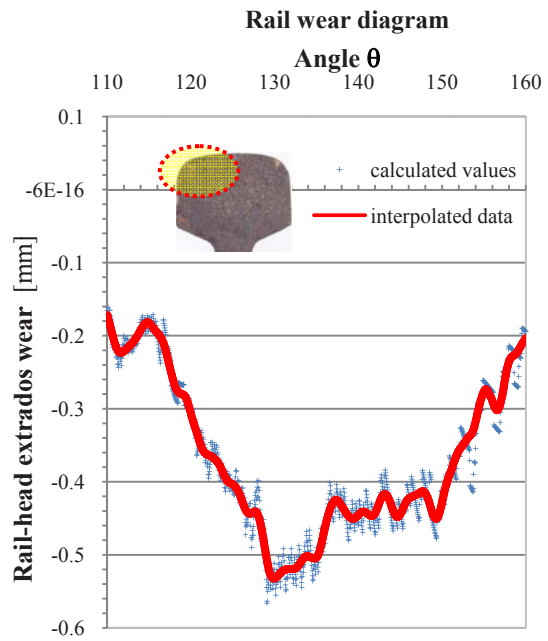


Fig.8. Grooved Rail wear diagram (Cartesian coordinate system, see Fig.6)

Fig. 9. UIC 60 Rail wear diagram ( $\theta = 20^\circ$ - $70^\circ$ )Fig. 10. UIC 60 Rail wear diagram ( $\theta = 110^\circ$ - $160^\circ$ )

#### 4. Conclusions

This research has examined a new procedure based on the *imageprocessingtechnique* for determining the rail wear on tramway track. This new non-conventional method, based on the analyses of high resolution photo images, has required the design and implementation of specific mathematical algorithms suitable to provide the cross section geometry of a generic worn-out rail and the measurements of its relevant deviations in comparison with new rails of the same type (Grooved rail and UIC 60 rail). At present, the procedure can be only used for the lab analyses showing high precision in the wear evaluation as well as great rapidity in being performed. So, it is very likely that a conventional laser monitoring system will be combined with a digital one in the future.

#### References

- [1] Esveld, C. (2001). Modern Railway Track-Second Edition. MRT Productions.
- [2] Alippi C., Casagrande E., Scotti F. and Piuri V. (2000). Composite Real-Time Image Processing for Railways Track Profile Measurement. IEEE Transactions on instrumentation and measurement, Vol. 49, n. 3.
- [3] Guerrieri M., Parla G. and Ticali D. (2012). Mono and Stereoscopic Image Analysis for Detecting the Transverse Profile of Worn-Out Rails. Procedia - Social and Behavioral Sciences. ISSN: 1877-0428 (SIIV 2012 “Sustainability of Road Infrastructures” Conference proceedings, 29-31 October 2012, Roma, Italy) – in press.
- [4] Guerrieri M., Parla G. and Ticali D. (2012). A theoretical and experimental approach to reconstructing the transverse profile of worn-out rails. Ingegneria Ferroviaria, January 2012, (pp. 23-37), ISSN: 0020-0956.
- [5] Guerrieri M., Ticali D. (2012). Sustainable mobility in park areas: the potential offered by guided transport systems. International Conference on Sustainable Design and Construction, March 23-25, 2011, Kansas City, Missouri, ASCE (2012). Volume: ICSDC 2011, Integrating Sustainability Practices in the Construction Industry, pp. 661-668, ISBN 9780784412046, ASCE Conf. Proc. doi:10.1061/41204(426)81.
- [6] Guerrieri M., Ticali D. (2012). Design standards for converting disused railway lines into greenways. International Conference on Sustainable Design and Construction, March 23-25, 2011, Kansas City, Missouri ASCE (2012). Volume: ICSDC 2011, Integrating Sustainability Practices in the Construction Industry, (pp. 654-660), ISBN 9780784412046, ASCE Conf. Proc. doi:10.1061/41204(426)80.
- [7] Canny J. (1986). A computational approach to edge detection. PAMI(8), No. 6, (pp. 679-698).
- [8] Gonzales R.C., Woods R. E. (2002). Digital Image Processing 2<sup>nd</sup> ed. Prentice Hall, Upper Saddle River, New Jersey.
- [9] Gonzales R.C., Woods R.E, Eddins S.L. (2004). Digital image processing using Matlab. Prentice Hall, Upper Saddle River (New Jersey).
- [10] Serra J. (1982). Image analysis and mathematical morphology. London, Academic Press.
- [11] Freeman, H., (1961). Computer Processing of Line Drawing Images. Computing Surveys. 6(1):57-97.
- [12] Trouillot X., Jourlin M., Pinoli J.C. (2008). Geometric parameters computation with freeman code. Submitted to Image anal stereol, 6 pages.
- [13] Corriere F., Di Vincenzo D. (2012). The Rail Quality Index as an indicator of the “Global Comfort” in optimizing Safety, Quality and Efficiency in Railway Rails. Procedia - Social and Behavioral Sciences. ISSN: 1877-0428 (SIIV 2012 “Sustainability of Road Infrastructures” Conference proceedings, 29-31 October 2012, Roma, Italy) – in press.
- [14] RFI (2002). Procedura operativa subdirezionale DMAIMSD P0 IFS 002 0 del 16.01.02, Rilievi della geometria del binario e relative disposizioni manutentive, Rete Ferroviaria Italiana (Italian Railway Network).